2014 IEEE/RSJ International Conference on
Intelligent Robots and Systems (IROS 2014)
September 14-18, 2014, Chicago, IL, USA

Variable Stiffness Fabrics with Embedded Shape Memory Materials for Wearable Applications

Thomas P. Chenal[1,2], Jennifer C. Case[1], Jamie Paik[3] and Rebecca K. Kramer[1*]

***Abstract*— Materials with variable stiffness have the potential to provide a range of new functionalities, including system reconfiguration by tuning the location of rigid links and joints. In particular, wearable applications would benefit from variable stiffness materials in the context of active braces that may stiffen when necessary and soften when mobility is required. In this work, we present fibers capable of adjusting to provide variable stiffness in wearable fabrics. The variable stiffness fibers are made from shape memory materials, where shape memory alloy (SMA) is coated with a thin film of shape memory polymer (SMP). The fibers, which are fabricated via a continuous feed-through process, reduce in bending stiffness by an order of magnitude when the SMP goes through the glass transition. The transition between rubbery and glassy state is accomplished by direct joule heating of the embedded SMA wire. We employ a COMSOL model to relate the current input to the time required for the fibers to transition between stiffness states. Finally, we demonstrate how this device can be worn and act as a joint stability brace on human fingers.**

I. Introduction

Systems and materials that can controllably change their stiffness are useful in a broad range of applications and have the potential to revolutionize human-robot interaction. In the context of traditional rigid robots, there is currently interest in variable stiffness springs that allow the system to actively soften [1], [2]. However, while the joints may be softened to some extent, the links are still rigid and unyielding. In the automotive industry, magnetorheological fluids have allowed variable stiffness by controlling magnetic particles dispersed into a fluid via magnetic fields. Applications of these fluids are extending into other fields, such as medical devices [3] and soft robotics [4].

A growing interest in soft robotics has led to an increased interest in variable stiffness of soft materials. Some recent examples of variable stiffness materials include soft robotic manipulators that operate using pneumatic particle jamming [5], [6], [7] or layer jamming [8]. These manipulators function via the loosening of particles or layers by removing a vacuum, thus allowing the robot to move; reapplication of the vacuum causes rigidity to be regained. Variable stiffness of elastomers has been achieved by embedding the elastomer with magnetic particles and altering the magnetic field around the polymer [9]. However, devices of this nature require external equipment, which limits the scalability and mobility of the integrated system. A more scalable solution has been achieved through use of elastomers embedded with low-melting-temperature-alloys; the alloy is melted either by direct heating [10] or with the use of an embedded heater [11], resulting in material compliance enabled by phase change.

Fig. 1. Top: Variable stiffness fabric curled into a spiral. Bottom: Variable stiffness fabric shaped into an oscillatory pattern.

Planar and conformable systems represent an intriguing new class of soft wearable robotics. Current work on actuated soft wearable systems includes active soft orthotic devices based on pnuematics [12], [13] and shape memory alloy [14], as well as a soft exosuit made from pneumatic actuators and inextensible webbing [15]. A major challenge in this emerging field is in designing integrated wearable systems that do not constrain the natural motions of the wearer. Along these lines, we believe that the future of wearable systems will include smart fabrics, as fabric is a readily available 2D platform that is conformable and heavily integrated into our everyday lives as a wearable material. Along with enhancing fabrics with actuation and sensing capabilities, many wearable applications will require variable stiffness materials to provide joint or wound stability as well. We envision wearable fabric-based active stability braces that may stiffen to stabilize a joint during exertion or injury, and soften to allow mobility and agility to the wearer.

In this work, we present variable stiffness fibers with integrated joule heating by combining shape memory alloy (SMA; nickel titanium [NiTi]) wire with shape memory polymer (SMP; polylactic acid [PLA]), where the NiTi wire is only used as the electrical heater for the polymer instead of a shape memory material. The resulting fibers are then sewn into a fabric to create a variable stiffness fabric, which may

*Author to whom correspondence should be addressed rebeccakramer@purdue.edu
[1]School of Mechanical Engineering, Purdue University, West Lafayette, IN 47907, USA
[2]Department of Materials Science and Engineering, Ecole Polytechnique Fédérale de Lausanne, 1015 Lausanne, Switzerland
[3]Department of Mechanical Engineering, Ecole Polytechnique Fédérale de Lausanne, 1015 Lausanne, Switzerland

be employed as an active wearable brace for joint stability. NiTi was chosen as the heating element due to its availability, high electrical and thermal conductance, as well as future plans to exploit the shape memory effect to develop variable stiffness actuators. PLA was chosen as the coating for its availability, ease of processing, and desirable glass transition temperature. Even though PLA has a shape memory effect, it is very weak and the polymer is not developed for this purpose, so for this work the PLA is used for its change in stiffness while going through the glass transition temperature.

II. Fabrication

A. Coated wire production

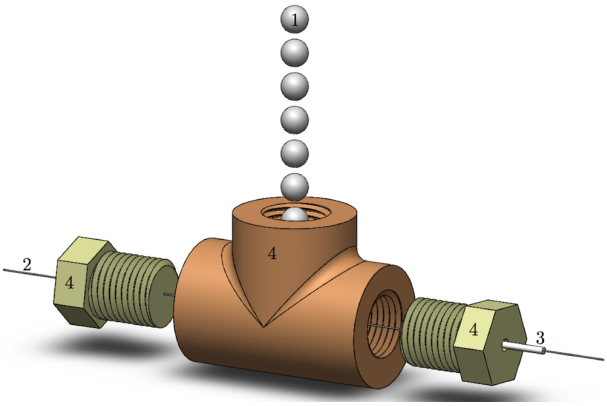

Fig. 2. Setup built for coating the SMA with a shape memory polymer (PLA). Polymer pellets (1) are melted onto SMA wire (2) to create a uniformly coated fiber (3) via a brass structure (4).

The setup used for the fiber fabrication is presented in Figure 2. It is made of a brass T-junction with both sides fitted with two bolts with pre-drilled holes. The diameter of the hole by the entrance of the SMA is close to the SMA wire diameter, while the exiting hole's diameter is sized to the desired PLA coated SMA wire diameter. The entire structure is heated on a hot plate to $200°C$, which is sufficiently higher than the melting temperature of the PLA ($T_m = 150°C$). Polymer pellets are fed into the top of the setup. When the polymer is melted, the SMA wire is pulled slowly through the setup manually. During the process, a constant feeding of polymer is maintained to achieve a quasi-continuous process and relatively uniform coating of PLA on SMA.

The overall diameter of the composite fiber can easily be tuned by varying the size of the exit hole, which will subsequently adjust the thickness of the polymer coating around the SMA. For the purpose of this work, the diameter of the fiber produced was held constant at approximately $1.2(\pm 0.1)$ mm with an inner NiTi wire diameter of 0.254 mm.

B. Variable stiffness fabric

After coating, the fibers are cut to a predefined length, here about 230 mm, and then sewn onto a piece of fabric to create a variable stiffness fabric. The produced fabric sample is shown in Figure 3. Figure 4 shows the stiffness variation potential of the fabric. The fabric used here is a black woven plain-weave of very thin polyester where the thickness is less than a tenth of a millimeter. Hence, the overall stiffness of the integrated fabric is provided by the SMA/PLA fibers. When the PLA is heated above its glass transition, the fabric can be easily deformed to any type of shape; as the polymer transitions back to the glassy state, the polymer stiffens to hold its shape, as seen in Figures 1 and 4. When reheated and under no external load, the fabric tends to go back towards its initial shape due to the slight memory effect of the PLA. However, this takes between $10 - 30$ seconds depending on the deformed shape and the input current, and it can never fully recover its original shape.

Fig. 3. Variable stiffness fibers sewn onto fabric.

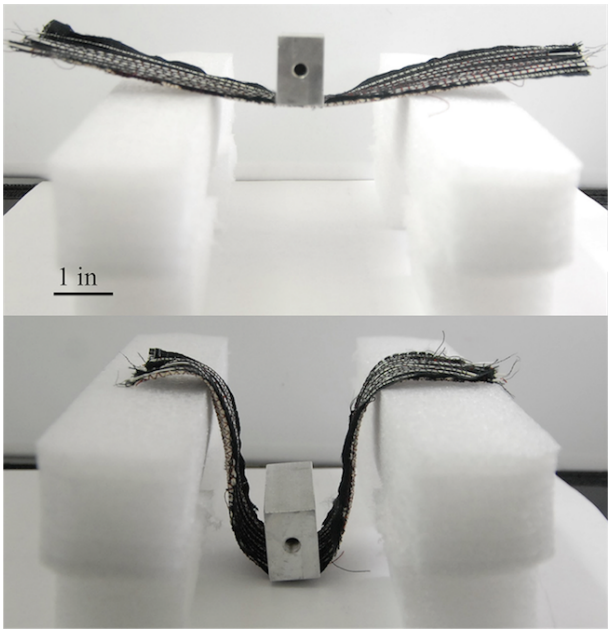

Fig. 4. Variable stiffness fabric in stiff (top) and soft (bottom) states. The mass shown in the image is 63.5 g.

III. Experiment

A. Material properties

The variable stiffness fibers all employ a 0.254 mm NiTi wire provided by Dynalloy, Inc. The majority of the PLA used was provided by Open Source Printing, LLC, which is transparent; exceptions include the PLA used for the fabric sample shown in Figure 3 where a PLA with white colorant was used. The PLA is used in this work as a variable stiffness material; when joule heated by the NiTi wire, it reaches the glass transition temperature, thereby transitioning

from glassy to rubbery state and thus, reducing its bending stiffness.

A differential scanning calorimetry (DSC) test was performed on the PLA. This test is a thermo-analysis technique that measures the difference in heat flux between the sample and a reference, usually air, as a function of the temperature. This allows us to determine the precise temperature of any physical transformation. The PLA sample was heated from room temperature to 300°C at 10°C/min. The resulting plot is shown Figure 5.

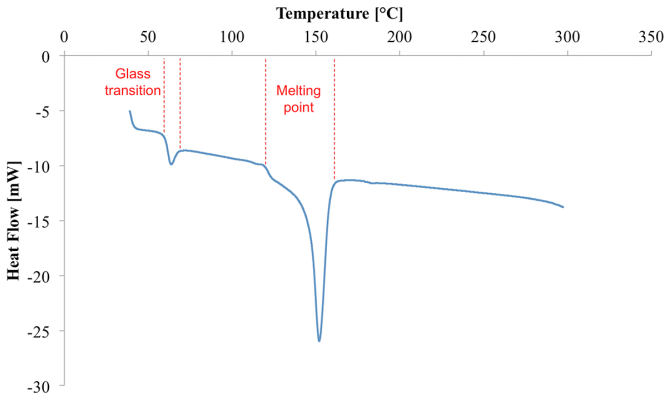

Fig. 5. Differential scanning calorimetry test of the PLA; tested on a PLA pellet.

B. COMSOL Simulation

A COMSOL simulation was performed to determine the thermal response of the fiber with a selection of different current values. The simulated fiber presented in Figure 6 had the same dimensions as the fibers described in the fabrication section. The SMA wire length was 150 mm with a PLA coating that is 120 mm long in the center. Based on the geometry of the wire, the simulation was performed using an axially symmetric model. The initial temperature of both the SMA and the polymer were set to $20°C$. The boundary conditions for the SMA and the PLA in direct contact with the were defined as convection and the boundary between the SMA and the PLA was considered to be perfect, meaning that the temperature gradient continues at the interface. Results for the COMSOL simulation are given in the next section.

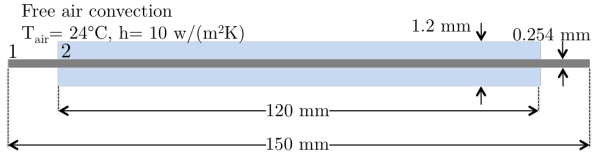

Fig. 6. Dimensions of a fiber comprised of NiTi SMA (1) and polymer coating (2).

C. Mechanical testing

Three point bending tests were performed on the single fibers and the whole fabric. The tests were performed on an Instron 3345 material testing machine with a 5 kN flexural fixture and a 50 N load cell. The setup can be seen in Figure 7. The samples tested were 120 mm long, with a diameter of approximately 1.2 mm. The support span was set at 40 mm for the single fiber test and at 50 mm for the fabric. The sample was loaded at 2 mm/min until the deflection reached 10 mm for the fiber and 8 mm for the fabric. Two tests were done on both the single fiber and the fabric: one with no input current and one with an input current of 0.60 A. Each test was performed three times for both the single fiber and fabric and the data from these runs were averaged together.

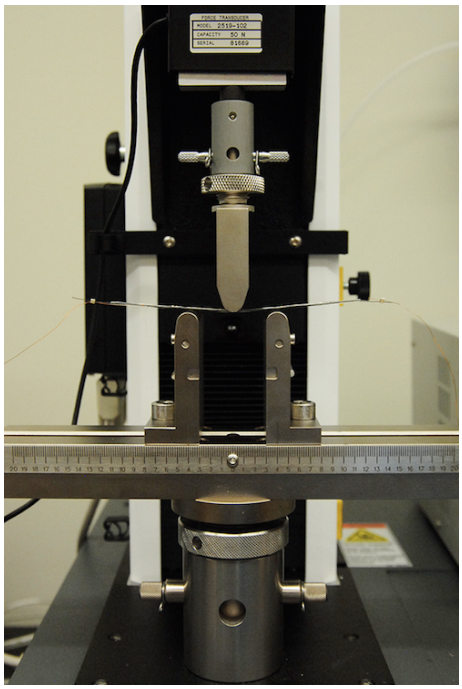

Fig. 7. Three point bending test setup.

IV. Results and Discussion

A. Material properties

The DSC test result in Figure 5 shows two endothermic events. The first one occurs at approximately 60°C and corresponds to the glass transition of the material. The second event occurs around 150°C and corresponds to the melting temperature of the PLA. This data is used in the COMSOL simulations to help determine the ideal current for heating the fibers.

B. COMSOL Simulation

Figure 8 shows that the heating speed and the final temperature is directly related with the input current. Figure 8(a) represents the thermal response of the outer surface at the center of the fiber. For the fiber to become completely soft, all of the PLA coating should go through the glass transition temperature, denoted by T_g on the graph. Based on the simulation, an input current greater than 0.32 A should fulfill this requirement. It should be noted that because this is a

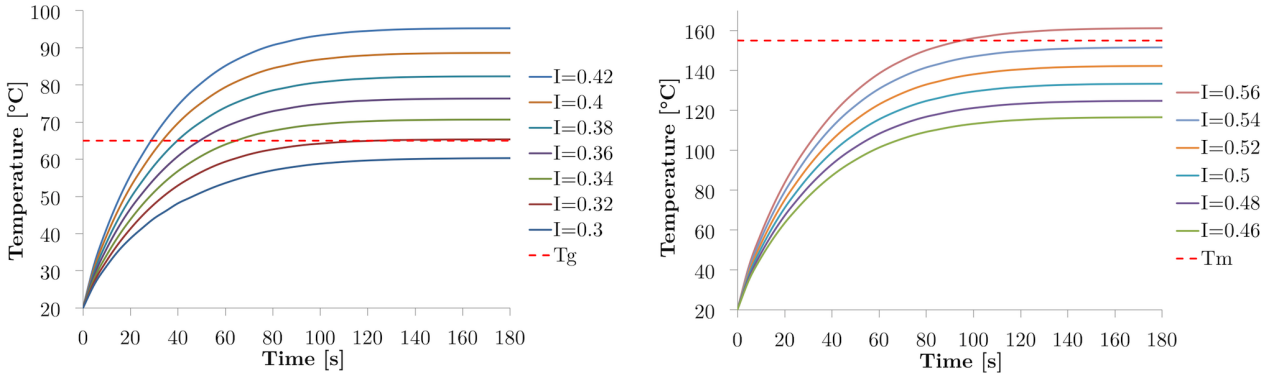

Fig. 8. COMSOL simulations for: (a) The outer surface at the center of the fiber from I=0.3 A to 0.42 A in 0.02 A increments. The dashed line indicates the glass transition temperature of PLA. (b) The PLA-SMA interface near the end of the fiber from I=0.46 A to 0.56 A in 0.02 A increments. The dashed line indicates the melting point of PLA.

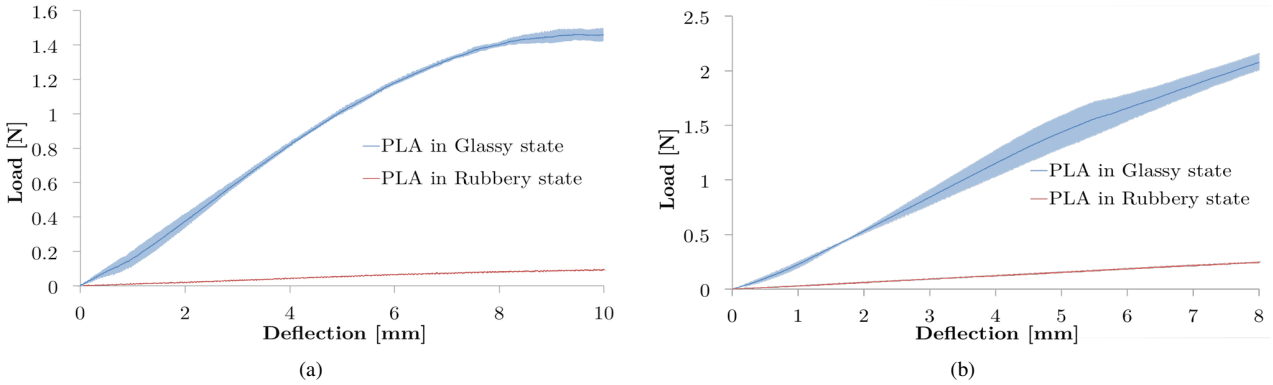

Fig. 9. Three point bending tests of the variable stiffness fiber (a) and the variable stiffness fabric, containing 10 individual fibers (b). Data represent the average of 3 tested samples, and shaded regions represent one standard deviation.

simulation, all materials are assumed to be free of impurities and interfaces are modeled as perfect, which may yield discrepancies in empirical testing. Experimentally, we found a current of 0.3 A was not enough to soften the fiber and that a current of at least 0.45 A had to be used in order to see a softening of the fiber.

Figure 8(b) represents the thermal response at the interface between the PLA and SMA near the end of the fiber. As shown in the graph, too high of an input current leads to a final temperature above the melting point, denoted by T_m, which can permanently damage the device by loosening the PLA from the SMA wires. It was observed experimentally that when the current was set too high, PLA would melt in the center and then recrystallize as the fiber cooled down, creating a non-transparent coloring in the fiber.

Based on the COMSOL simulation, an input current of 0.54 A is the best choice to reach the glass transition as fast as possible without any risk of melting the PLA. With this input current, the PLA coating should reach a rubbery state in less than 15 s. Due to the impurities that exist in the actual fibers, an input current of 0.60 A was used during testing, which yielded a rubbery state in less than 15 s, as predicted in the simulation.

C. Mechanical testing

Material resistance to deflection, as measured by the three point bending tests, for both the single fiber and fabric is shown in Figure 9. It can be seen from Figure 9(a) that the transition of the PLA from glassy to rubbery state induces a drop in the bending resistance by more than 10 times in a single fiber. For the test in the glassy state, two behaviors can be seen in the results: one for the elastic state and one for the plastic state. The elastic state corresponds to the linear behavior at the beginning of the curve. The material enters plastic state when the linear behavior ends. In the rubbery state, the material stays in the elastic state within the entire deformation range. The mechanical behavior of the fabric is similar to that of the single fiber. However, due to the smaller final deformation and larger span distance, both curves stay in the elastic state. In the future this deflection data can be used to determine the stiffness of the fibers/fabric by obtaining the flexural modulus of the composite material.

V. Variable Stiffness Fabric Application

Figure 10 demonstrates the wearability of the variable stiffness fabric. When the PLA is in a glassy state, the fabric prevents movement around the joints, keeping the fingers in

a given position. This state can be used to support a joint during the recovery of an injury. When joint movement is needed, the fabric can be heated. This softens the fabric to allow for movement. To lock the fabric in place again, the current can be powered off and cooled down by the surrounding environment. It should be noted that based on both the COMSOL simulation and thermal imaging, the maximum temperature felt at the skin was around $48°C$. At this temperature the exposure time must be limited to 40 seconds to prevent acute and minor skin burns [16]. During our experiments, heating and reconfiguration cycles where consistently under 40 seconds and no user discomfort was noticed.

Fig. 10. Demonstration of the variable stiffness fabric on a finger joint. Heating and cooling of embedded variable stiffness fibers allows the fabric to change configuration or rigidly hold its shape, respectively.

VI. Conclusion and Future work

We have developed a new, fast, and simple way of producing thermally activated variable stiffness fabrics with embedded heaters by coating SMA wire with PLA and sewing the resulting fibers onto the fabric. The fabric presented here demonstrates an order of magnitude change in bending stiffness within less than 15 s when the PLA goes through the glass transition. This technology has high potential in robotics applications and especially in wearable devices, as demonstrated.

Future work will look at integrating these variable stiffness fibers with programmed SMA. This means that the SMA will pull the fibers to a given position, while the PLA will lock that position in place until the fibers are reheated. Future work will also focus on the fabrication of these fibers to improve precision and consistency. The fibers can also be improved by replacing the PLA with another SMP that has a lower glass transition temperature, which would reduce the response time of the fibers.

Acknowledgment

The authors would like to thank Malina Padgett from the Apparel Design and Technology Major at Purdue University for her help with the fabric integration. They are also very grateful to Prof. Jeffrey Youngblood and Gamini Mendis from the Department of Material Engineering at Purdue for letting us use their DSC machine.

References

[1] Sebastian Wolf and Gerd Hirzinger. A new variable stiffness design: Matching requirements of the next robot generation. In *Robotics and Automation, 2008. ICRA 2008. IEEE International Conference on*, pages 1741–1746. IEEE, 2008.

[2] Gill A Pratt and Matthew M Williamson. Series elastic actuators. In *Intelligent Robots and Systems 95.'Human Robot Interaction and Cooperative Robots', Proceedings. 1995 IEEE/RSJ International Conference on*, volume 1, pages 399–406. IEEE, 1995.

[3] J Z Chen and W H Liao. Design, testing and control of a magnetorheological actuator for assistive knee braces. *Smart Materials and Structures*, 19(3):035029, 2010.

[4] Carmel Majidi and Robert J. Wood. Tunable elastic stiffness with microconfined magnetorheological domains at low magnetic field. *Applied Physics Letters*, 97(16):–, 2010.

[5] J.R. Amend, Brown Jr., N. E., Rodenberg, H. Jaeger, and H. Lipson. A positive pressure universal gripper based on the jamming of granular material. *IEEE Transactions on Robotics*, 28:341–350, Apr. 2012.

[6] E. Steltz, A. Mozeika, N. Rodenberg, E. Brown, and H.M. Jaeger. JSEL: jamming skin enabled locomotion. In *IEEE/RSJ International Conference on Intelligent Robots and Systems, 2009. IROS 2009*, pages 5672–5677, 2009.

[7] N.G. Cheng, M.B. Lobovsky, S.J. Keating, A.M. Setapen, K.I. Gero, A.E. Hosoi, and K.D. Iagnemma. Design and analysis of a robust, low-cost, highly articulated manipulator enabled by jamming of granular media. In *2012 IEEE International Conference on Robotics and Automation (ICRA)*, pages 4328–4333, 2012.

[8] Yong-Jae Kim, Shanbao Cheng, Sangbae Kim, and Karl Iagnemma. Design of a tubular snake-like manipulator with stiffening capability by layer jamming. In *Intelligent Robots and Systems (IROS), 2012 IEEE/RSJ International Conference on*, pages 4251–4256. IEEE, 2012.

[9] Zsolt Varga, Genovéva Filipcsei, and Miklós Zrínyi. Magnetic field sensitive functional elastomers with tuneable elastic modulus. *Polymer*, 47(1):227–233, 2006.

[10] Bryan E. Schubert and Dario Floreano. Variable stiffness material based on rigid low-melting-point-alloy microstructures embedded in soft poly(dimethylsiloxane) (pdms). *RSC Adv.*, 3:24671–24679, 2013.

[11] Wanliang Shan, Tong Lu, and Carmel Majidi. Soft-matter composites with electrically tunable elastic rigidity. *Smart Materials and Structures*, 22(8):085005, 2013.

[12] Yong-Lae Park, Bor-rong Chen, Diana Young, Leia Stirling, Robert J Wood, Eugene Goldfield, and Radhika Nagpal. Bio-inspired active soft orthotic device for ankle foot pathologies. In *Intelligent Robots and Systems (IROS), 2011 IEEE/RSJ International Conference on*, pages 4488–4495. IEEE, 2011.

[13] Daniel P Ferris, Joseph M Czerniecki, Blake Hannaford, et al. An ankle-foot orthosis powered by artificial pneumatic muscles. *Journal of Applied Biomechanics*, 21(2):189, 2005.

[14] Leia Stirling, Chih-Han Yu, Jason Miller, Elliot Hawkes, Robert Wood, Eugene Goldfield, and Radhika Nagpal. Applicability of shape memory alloy wire for an active, soft orthotic. *Journal of materials engineering and performance*, 20(4-5):658–662, 2011.

[15] Michael Wehner, Brendan Quinlivan, Patrick M Aubin, Ernesto Martinez-Villalpando, Michael Baumann, Leia Stirling, Kenneth Holt, Robert Wood, and Conor Walsh. A lightweight soft exosuit for gait assistance. In *Robotics and Automation (ICRA), 2013 IEEE International Conference on*, pages 3362–3369. IEEE, 2013.

[16] P. S. Yarmolenko, E. J. Moon, C. Landon, A. Manzoor, D. W. Hochman, B. L. Viglianti, and M. W. Dewhirst. Thresholds for thermal damage to normal tissues: An update. *Int J Hyperthermia*, 2011.